Journal of the Korean Physical Society, Vol. 52, No. 2, February 2008, pp. 386∼390

Observation of a Spin-Singlet Proximity Effect in a Superconductor/Ferromagnet Interface

Dong-Keun Ki and Hu-Jong Lee*
Department of Physics, Pohang University of Science and Technology, Pohang 790-784

(Received 15 November 2007)

Since a spin-singlet superconductor (SC) and a ferromagnet (FM) have ground states with conflicting spin configurations, the superconducting order in a FM in proximity contact with a SC is bound to be suppressed. However, a rather long-range proximity effect has been observed in a metallic FM of a SC/FM junction. Recently, the possible formation of long-range spin-triplet pairing at the SC/FM interface has also been claimed. In this study, we examined the superconducting proximity effect in a simple spin-singlet SC/FM interfacial structure, where the formation of long-range spin-triplet pairing was highly unlikely. We suggest that the finite resistance reduction of the FM segment observed in this study due to the proximity contact to a SC is explicable by the ordinary short-range spin-singlet proximity effect combined with a current redistribution through the SC overlay due to the Andreev reflection at the interface of the unpolarized electrons in the FM.

PACS numbers: 74.50.+r, 74.25.Fy, 74.23.-b
Keywords: Proximity effect, Superconductor/Ferromagnet interface, Coherence length, Triplet superconductivity

I. INTRODUCTION

The formation of an order in an interface between two materials with incompatible ground states is of particular interest. The superconducting proximity effect in a superconductor (SC)/ferromagnet (FM) interface is such an example, where the superconducting ground state consists of a spin-singlet paired state while in the ferromagnetic ground state spins are aligned. The spin-singlet superconducting order in the FM of a SC/FM interface is expected to survive only over a microscopic length $\xi_m = \sqrt{\hbar D/E_{ex}}$ (E_{ex}: the exchange energy of a FM). For a conventional metallic FM such as permalloy (Py) or cobalt (Co), the coherence length becomes at best ∼1 – 2 nm, which is too short for the proximity properties to be conveniently probed experimentally. Due to this very conflicting nature of the order parameters, a SC/FM interface exhibits rich physical phenomena, like an oscillating [1] and a possible long-range spin-triplet [2] superconducting order in the FM. The former has been studied extensively, which reveals the non-monotonic thickness dependence of the transition temperature, the 0-π-junction transition of the Josephson effect, and the abnormal tunneling density of states [1]. In the meantime, the long-range spin-triplet pairing state has been proposed recently, on which a lot less experimental investigation has been carried out [3,4].

In a junction between a spin-singlet SC and a magnetic system, the proximity superconducting order extends longer into the magnetic system for weaker magnetic strength, which was clearly demonstrated in a SC/Kondo-wire bilayer system [5]. In contradiction to the general expectation, however, even in a simple interfacial structure between a SC and a strong FM, a large resistance reduction was observed and was interpreted in terms of an unidentified strong proximity effect [6]. Ensuing theoretical and experimental studies, however, ascribed the reduction of the resistance to an artifact such as the domain-wall motion or the redistribution of the current at the interface [7–9]. In the current-redistribution model, the resistance reduction was assumed to be mainly due to shunting of the current through the SC at the SC/FM interface [8]. In this picture, however, the opening of a quasiparticle energy gap in the SC, which would have prevented polarized normal electrons (or quasiparticles) from shunting through the SC for a subgap bias, was not taken into account [10].

To examine the validity of the proximity-related interpretation of the observed resistance reduction in a SC/FM interface, we fabricated a simple bilayer structure, as shown in Figure 1(a). The sample consists of two segments in a single FM (Py) wire, where one was in contact with a SC (with corresponding potential difference of V_{FS}), but no contact with a SC was made for the other segment (corresponding to V_F). We probed the super-

*E-mail: hjlee@postech.ac.kr

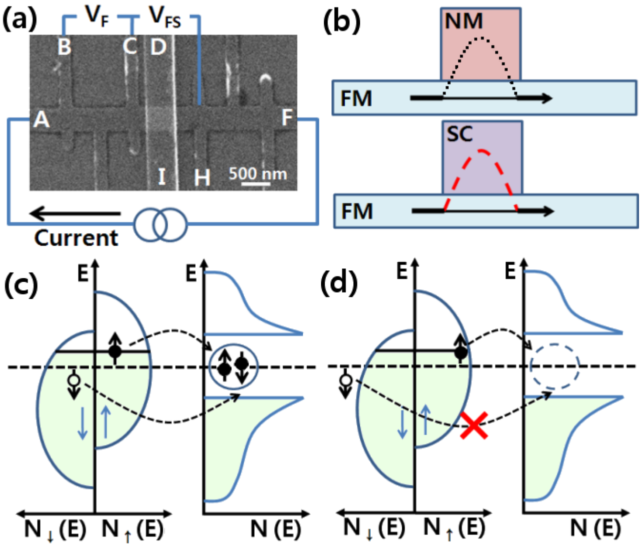

Fig. 1. (a) Sample geometry and the measurement configuration. The vertical lighter stripe is a niobium (Nb) overlay employed as a superconducting electrode, and the horizontal darker stripe is a permalloy (Py) layer employed as a ferromagnet (FM) channel. (b) Schematics of the current redistribution in a FM in proximity contact with a normal metal (upper) and a superconductor (lower). The dotted (broken) line in the upper (lower) drawing represents a normal shunting current (a supercurrent) through the Nb overlay in its normal (superconducting) state. (c) An allowed Andreev-reflection process. When a FM has a finite current polarization p, a $1-p$ part of the total current can be shunted through the superconductor while forming Cooper pairs. (d) A forbidden Andreev-reflection process. A fraction p of the total current cannot be shunted through the superconductor because no states are available to form Cooper pairs.

conducting proximity effect by measuring and comparing the resistance of the SC-contacted FM segment with that of the FM segment without a SC contact as a function of temperature and bias current. The aspect ratio of the FM layer was designed to be large enough to make it single-domain-like so as to rule out the possibility of the formation of the spin-triplet pairing state. A significant resistance reduction was observed in the proximity-contact ferromagnetic segment. We show that it can be analyzed in terms of the short-range spin-singlet proximity effect along with a simple Andreev-reflection-related supercurrent shunting through the SC overlay.

II. FABRICATION AND MEASUREMENT

A SC/FM proximity junction was fabricated using multiple e-beam lithography and deposition processes. We first deposited a 500-nm-wide and 15-nm-thick Py ferromagnetic layer on an oxidized silicon-wafer substrate, followed by the cross deposition of a 500-nm-wide and 100-nm-thick Nb superconducting overlay, both by using an e-beam patterning and lift-off technique. Before we deposited the Nb overlay, the surface of the Py layer was cleaned by irradiation with a low-energy Ar-ion beam for 30 seconds at a power of 2.5 W.

The scanning electron microscope (SEM) image of the sample is shown in Figure 1(a). Sample was mounted in a dilution fridge with a base temperature of 100 mK. Each electrical measurement lead was connected to a low-pass π filter with 5-dB attenuation at 10 MHz. A lock-in amplifier (Stanford Research; SR830) was used to take the differential resistance of the sample in a four-probe configuration [see Figure 1(a)]. Unless stated otherwise, the bias current was applied through leads A and F. The R vs T curve was taken for a 1-μA ac bias current with a frequency of 13.3 Hz while a 0.1-μA modulation with the same frequency was used to take the differential resistance in conjunction with a WaveTek 184 function generator for the dc bias sweep.

III. RESULTS AND DISCUSSION

As the temperature is lowered across the superconducting transition temperature T_c from above, the resistance R_{AFCH} (=V_{FS}/I) of the ferromagnetic Py segment in contact with the SC decreases from 31.9 Ω to 29.4 Ω ($\Delta R_{exp} \approx 2.5$ Ω) while the resistance of the neighboring segment of the same length, but without the contact with a SC, R_{AFBC} (=V_F/I), remains the same at 46.8 Ω [see Figure 2(a)]. At higher temperatures around 8.5 K, R_{AFCH} is smaller than R_{AFBC}, which is due to the current redistribution effect to be discussed below. Figure 2(a) clearly indicates the appearance of the superconducting proximity effect in the Py segment. In addition, the contact resistance R_{DFIA} (=V_{IA}/I_{DF}) is negative when the Nb is in the normal state, but it becomes positive as Nb turns superconducting. The contact resistances in different measurement configurations, R_{DFIA}, R_{FDAI}, R_{IADF} and R_{AIFD}, show identical values, which indicates that the negative contact resistance was not caused by the nonuniformity of the interfacial resistance distribution itself over the junction. The negative resistances in the normal state of Nb, on the other hand, indicate that the contact resistance was less than the normal-state sheet resistances of both the Nb and the Py layers, which led to a nonuniform current distribution even for a uniform interfacial resistance at the junction.

Figure 2(b) shows the bias current dependence of the differential resistance at the base temperature of 100 mK. In the low-bias region the differential resistance of the SC-contacted Py segment (AFCH) is reduced below the one at a high-enough bias current. In contrast, the resistance of the Py segment without a SC contact (AFBC) does not change. The contact resistance (DFIA) changes from positive to negative as the bias current is increased. The current value giving the pronounced peak (Peak 1) in the differential resistance should be the critical cur-

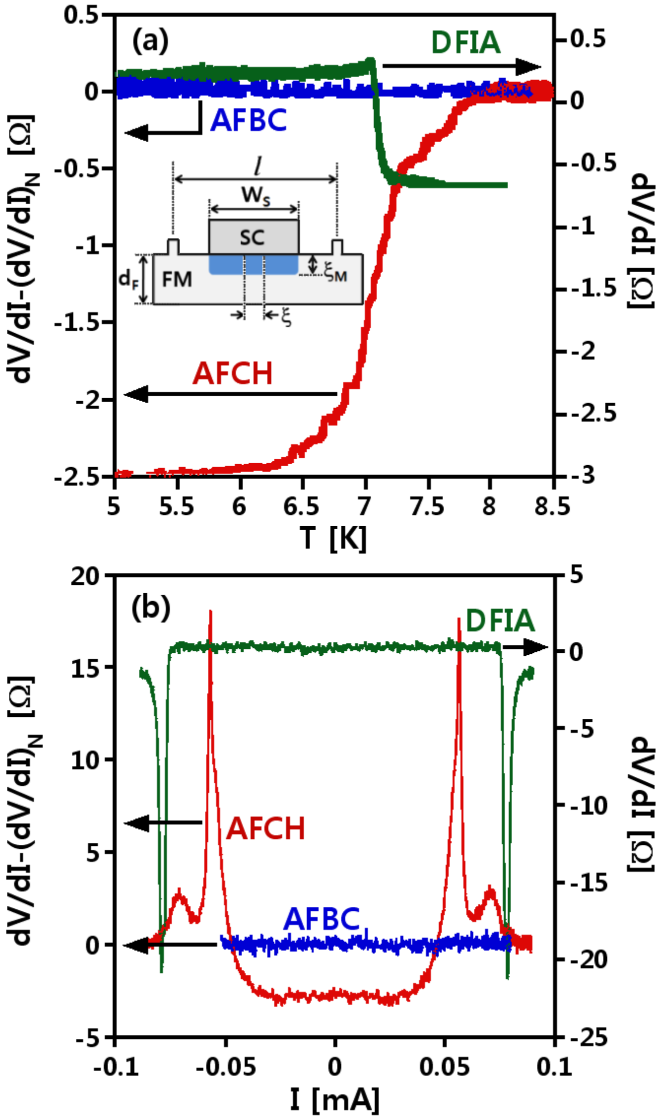

Fig. 2. (a) Temperature dependence of the resistance. The left vertical axis represents the resistance difference from the value at 8.5 K ($T > T_c$) while the right axis is the resistance itself. The label AFCH, for instance, stands for the measurement configuration where the current is applied through leads A and F and the voltage difference [V_{FS}] is measured between leads C and H. Thus, the configuration DFIA gives the change in the contact resistance between the Nb and the Py electrodes. The inset illustrates the schematic geometry of the sample. W_S is the width of the Nb overlay under which the proximity effect penetrates vertically into the FM up to ξ_m and l is the spacing between two voltage leads. ξ is the length in the FM over which the proximity effect modifies the resistance of the FM segment under the assumption that the superconducting coherence penetrates over the whole thickness of the FM segment. (b) Differential resistance of different configurations as a function of bias current at 100 mK with no magnetic field applied. The notations for the measurement configurations are the same as in (a).

rent of the proximity-induced superconducting region in

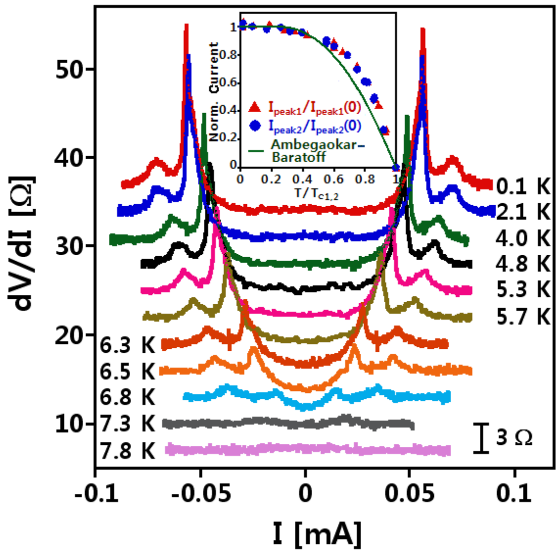

Fig. 3. Temperature dependence of dV/dI vs I (each curve is shifted vertically by 3 Ω for clarity). The inner peak reduces to zero at 7.3 K while the outer peak vanishes at 7.8 K. Inset: The normalized current positions of the peaks as a function of normalized temperature. All points merge into a single curve and follow the Ambegaokar-Baratoff relation well.

the Py segment. In Figure 2(b), one also finds a minor peak (Peak 2) at a higher bias, the cause of which is not well understood.

As the temperature is increasesd, Peak 1 vanishes at 7.3 K while Peak 2 survives until 7.8 K (Figure 3). The vanishing temperatures are close to the superconducting critical temperature of a slightly disordered Nb electrodes. The normalized temperature dependencies of the two peaks, shown in the inset of Figure 3, merge into a single curve, which follows the Ambegaokar-Baratoff-type temperature dependence of the critical current well [11]. Thus, Figure 3 indicates that both peaks are caused by the proximity contact of a FM with a SC.

Using the resistance decrease of $\Delta R_{exp} \approx 2.5$ Ω obtained from both the R vs T and the dV/dI vs I curves for the 1-μm-long (l) Py segment in contact with the Nb overlay, in comparison with that in reference to the resistance of the Py segement of the same length without a Nb contact ($R_{AFBC} = 46.8$ Ω), we estimate the proximity length (ξ) as

$$\xi = l \times \frac{\Delta R_{\rm exp}}{R_{AFBC}} = 53.4 \text{ nm}. \quad (1)$$

This value turns out to be much longer than the value of the coherence length expected for an ordinary FM. In this calculation, the whole thickness of the FM located underneath the SC of width W_S is assumed to be affected by the superconducting proximity effect [see the inset of Figure 2(a)], which is the usual situation in the normal-metal (NM) at a SC/NM proximity junction. In reality, however, the superconducting coherence length is likely to be shorter than the thickness of the FM layer. Since the resistance modified by the proximity effect is supposed to depend on the proximity-affected volume of the FM the relation $\xi \times d_F = \xi_m \times W_S$ should hold [see the inset of Figure 2(a)]. Then, the actual coherence length (ξ_m) is estimated to be

$$\xi_m = \xi \times \frac{d_F}{W_S} = 53.4 \text{ nm} \times \frac{15 \text{ nm}}{500 \text{ nm}} = 1.6 \text{ nm}, \quad (2)$$

which is in the range of $\sqrt{\hbar D/E_{ex}}$.

However, as mentioned above, R_{AFCH} differs from R_{AFBC} even in the normal state for $T>T_c$. This is because a part of the current diffused into the Nb overlay owing to the small contact resistance between the two materials [see the upper panel of Figure 1(b)]. As a result, the amount of the resistance reduction used above to estimate ξ_m should be re-estimated. For the subgap-bias region in the superconducting state of the Nb overlay, quasiparticles are not able to pass through the SC due to an opening of the energy gap so that only the supercurrent constituted the shunting current in Nb, which was generated by the Andreev reflection process [10] [see the lower panel of Figure 1(b)]. Thus, the reference for the actual resistance reduction (ΔR_{real}) should be the resistance of the Py segment not in contact with the SC (AFBC) rather than that of the Py segment in contact with the SC. The corresponding resistance reduction is 17.4 Ω [=($R_{AFBC} - R_{AFCH}$) at 4.2 K], rather than 2.5 Ω, which leads to a coherence length of 11.1 nm [=370 nm × (d_F/W_S)], ∼7 times longer than the simple estimate in Eq. (2).

To explain this large proximity effect, we first consider the possibility of the formation of an odd-frequency spin-triplet pairing state at the SC/FM interface, which was recently proposed theoretically and was claimed to have been observed in a few experiments [2–4]. According to the theory, the spin-triplet superconducting order in a FM can survive over a macroscopic length ($\xi_N = \sqrt{\hbar D/k_B T}$) [2] if the FM has an inhomogeneously magnetized region like a domain wall or a spiral magnetic moment. In our samples, however, none of these conditions were met because we used a single FM layer with a high aspect ratio of over 20 [the width was 0.5 μm and the length over 10 μm]. In this case, the shape anisotropy energy forces the magnetization to point along the length direction of the layer, which leads to a single-domain structure [12].

However, as we see from the SEM image of our sample [Figure 1(a)], domain walls are likely to be created at the cross-sections between the voltage probes and the central ferromagnetic Py layer. In addition, a sufficiently dense spin-polarized current can move these domain walls or switch the magnetization [13,14] toward the region of the SC/FM interface to act as inhomogeneous magnetization regions. In our experiment, however, the highest current density applied was 10^{10} A/m^2, which was significantly smaller than the current density needed to move domain walls, 10^{12} A/m^2, as obtained in a real-time magnetic force microscope (MFM) measurement [13]. Thus, the possibility of domain-wall movement is negligibly low. All these lead to a conclusion that the spin-triplet picture cannot explain the observed large resistance reduction in the SC-contacted FM segment.

At this point, it should be mentioned that the long coherence length of 11.1 nm obtained above was estimated assuming that the bias current flow was uniform through the FM layer. However, the current uniformity should not have been maintained because of the current shunting through the SC overlay, where a simple estimate of the coherence length based on the resistance reduction was not possible. In this sense, the above-estimated coherence length is not of strict physical significance, except for reconfirming that the range of penetration of the superconducting order into the FM was shorter than the thickness of the FM layer. We will, thus, examine the validity of the establishment of the proximity effect at the SC/FM interface, as revealed in the large resistance change of the FM segment with the SC overlay, in terms of current shunting rather than in terms of the range of penetration of the superconducting coherence into the FM layer.

A large resistance reduction was also observed previously in other measurements, but without proper interpretation [6]. However, in Ref. 8, it was suggested that simple current shunting through the SC on top of the FM could explain the observed anomaly. In that interpretation, however, the opening of a quasiparticle energy gap in the SC was not taken into account. Since the shunting current through the SC should be a supercurrent the Andreev-reflection process at the SC/FM interface should be considered when analyzing the observed resistance reduction.

Figures 1(c) and (d) show the schematics of the Andreev-reflection process, where process (c) is allowed, but the process (d) is forbidden. For the allowed process, an electron forms a Cooper pair with another electron with the opposite energy, momentum, and spin, called Andreev reflection, even in the presence of an energy gap preventing normal electrons from entering into the SC. Therefore, in a FM/SC junction consisting of a partially polarized FM layer, the unpolarized portion of the total current $(1-p)$ [p: the current polarization factor] can diffuse into the SC because electrons in the portion can find pairing partners [Figure 1(c)]. Here, the total current I can be expressed as a sum of the polarized and the unpolarized components as

$$I = I_\uparrow + I_\downarrow = pI + (1-p)I, (p = \frac{I_\uparrow - I_\downarrow}{I_\uparrow + I_\downarrow}). \quad (3)$$

In this model, the maximum reduction factor of resistance with respect to the normal resistance should be $1-p$, which is 0.56 – 0.58 using the reported value of p in permalloy (=0.42 – 0.44) [15]. The ratio obtained from our measurements

$$(\frac{\Delta R_{exp}}{R_F^0})_{observed} \approx 0.74, \quad (4)$$

turns out to be close to the estimated value of $1-p$, where the resistance of the Py segment located underneath the SC, R_F^0, is about one half R_{AFBC}. This analysis indicates that the resistance reduction in the Py segment in contact with a SC is caused by the ordinary spin-singlet proximity effect, together with the supercurrent shunting of the unpolarized portion of the bias current due to the Andreev reflection through the SC from a partially polarized FM. The observed increase of the interfacial resistance R_{DFIA}, for instance, also indicates that the spin accumulation took place as only the $1-p$ fraction of the interfacial current was allowed to flow by the Andreev reflection upon transiting to the superconducting state of the Nb overlay.

This study illustrates that the resistance reduction of a FM segment with a partial spin polarization in a SC/FM bilayer due to superconducting proximity effect occurs in a different manner from that of a nonmagnetic normal metal (NM) segment in a SC/NM bilayer. In the latter, with an $\sim \mu$m-long proximity coherence length, the resistance reduction is usually determined by a portion twice the lateral extension of the proximity-induced superconducting region (*i.e.*, twice the coherence length) plus the lateral size of the SC electrode. However, in the former, the coherence length is usually even shorter than the thickness of the FM layer. In this case, the resistance reduction of the FM segment affected by the superconducting proximity effect is determined by the supercurrent shunting through the SC overlay rather than by the propagation of the superconducting order along the thickness of the FM layer underneath the SC overlay. Thus, if the SC width occupies a large fraction of the FM segment, even the short-range spin-singlet proximity effect can reveal itself in a significant resistance change of the FM segment, as in our study.

ACKNOWLEDGMENTS

This work was supported by the Electron Spin Science Center at POSTECH and by a Pure Basic Research Grant, R01-2006-000-11248-0, administered by the Korea Science and Engineering Foundation (KOSEF), and by a Korea Research Foundation grant, KRF-2005-070-C00055.

REFERENCES

[1] A. Buzdin, Rev. Mod. Phys. **77**, 935 (2005) and references therein.
[2] F. S. Bergeret, A. F. Volkov and K. B. Efetov, Rev. Mod. Phys. **77**, 1321 (2005).
[3] R. S. Keizer, S. T. B. Goennenwein, T. M. Klapwijk, G. Miao, G. Xiao and A. Gupta, Nature **439**, 825 (2006).
[4] I. Sosnin, H. Cho, V. T. Petrashov and A. F. Volkov, Phys. Rev. Lett. **96**, 157002 (2006).
[5] J. Eom, Y.-S. Shin, H.-J. Lee, D.-K. Kie, T. Kim and J. Song, J. Korean Phys. Soc. **48**, 446 (2006).
[6] V. T. Petrashov , I. A. Sosnin, I. Cox, A. Parsons and C. Troadec, Phys. Rev. Lett. **83**, 3181 (1999); M. D. Lawrence and N. Giordano, J. Phys.: Condens. Matter. **8**, L563 (1996); **11**, 1089 (1999); M. Giroud, H. Courtois, K. Hasselbach, D. Mailly and B. Pannetier, Phys. Rev. B **58**, R11872 (1998).
[7] S. V. Dubonos, A. K. Geim, K. S. Novoselov and I. V. Grigorieva, Phys. Rev. B **65**, R220513 (2002).
[8] W. Belzig, A. Brataas, Y. V. Nazarov and G. E. W. Bauer, Phys. Rev. B **62**, 9726 (2000).
[9] J. Aumentado and V. Chandrasekhar, Phys. Rev. B **64**, 054505 (2001).
[10] G. E. Blonder, M. Tinkham and T. M. Klapwijk, Phys. Rev. B **25**, 4515 (1982).
[11] M. Tinkham, *Introduction to Superconductivity*, 2nd ed. (Dover Publications Inc., New York, 1996).
[12] E. C. Stoner and E. P. Wohlfarth, Philos. Trans. London Ser. A **240**, 599 (1948).
[13] A. Yamaguchi, T. Ono, S. Nasu, K. Miyake, K. Mibu and T. Shinjo, Phys. Rev. Lett. **92**, 077205 (2004).
[14] J. H. Kong, S. Kim, Y. D. Park and K. Char, J. Korean Phys. Soc. **46**, 931 (2005).
[15] R. J. Soulen, Jr., J. M. Byers, M. S. Osofsky, B. Nadgorny, T. Ambrose, S. F. Cheng, P. R. Broussard, C. T. Tanaka, J. Nowak, J. S. Moodera, A. Barry and J. M. D. Coey, Science **282**, 85 (1998).